PROCEEDINGS OF SCIENCE

Electroweak box diagram contribution for pion and kaon decay from lattice QCD

Jun-Sik Yoo,[a,*] Tanmoy Bhattacharya,[a] Rajan Gupta,[a] Santanu Mondal[b] and Boram Yoon[c]

[a] *Los Alamos National Laboratory, Theoretical Division T-2, Los Alamos, New Mexico 87545, USA*
[b] *ArcVision Technologies, 34 Mahatma Gandhi Road, Kolkata 700009, India*
[c] *NVIDIA Corporation, Santa Clara, CA 95051, USA*
E-mail: junsik@lanl.gov, tanmoy@lanl.gov, rajan@lanl.gov, santanu.sinp@gmail.com, byoon@nvidia.com

One of the sensitive probes of physics beyond the standard model is the test of the unitarity of the Cabbibo-Kobyashi-Maskawa (CKM) matrix. Current analysis of the first row is based on $|V_{ud}|$ from fifteen superallowed $0^+ \to 0^+$ nuclear β decays and $|V_{us}|$ from the kaon semileptonic decay, $K \to \pi \ell \nu_\ell$. Modeling the nuclear effects in the $0^+ \to 0^+$ decays is a major source of uncertainty, which would be absent in neutron decays. To make neutron decay competitive requires improving the measurement of neutron lifetime and the axial charge, as well as the calculation of the radiative corrections (RC) to the decay. The largest uncertainty in these RCs comes from the non-perturbative part of the γW-box diagram, and lattice QCD provides a first principle method for its evaluation. Our calculations, using lattice configurations generated with highly improved staggered quarks by the MILC Collaboration, show that analogous calculations for the pion and kaon decays are robust and give $\square^{VA}_{\gamma W}|_\pi = 2.810(26) \times 10^{-3}$ and $\square^{VA}_{\gamma W}\Big|_{K^{0},SU(3)} = 2.389(17) \times 10^{-3}$ in agreement with the previous analysis carried out by Feng *et al.* using a different discretization of the fermion action.

The 40th International Symposium on Lattice Field Theory (Lattice 2023)
July 31st - August 4th, 2023
Fermi National Accelerator Laboratory

[*] Speaker

PoS(LATTICE2023)257

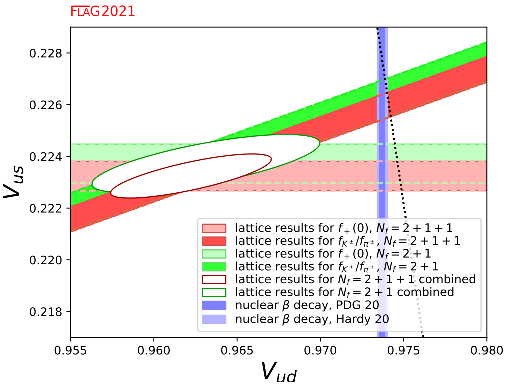

Figure 1: Current status of the unitarity bound taken from the FLAG report 2021 [5]

1. Introduction

In the intensity frontier, physics beyond the standard model (BSM) is probed by confronting accurate predictions of the standard model (SM) with precision experiments. Today, there are several tests showing roughly 2–3σ deviations, one being the unitarity of the first row of the CKM quark mixing matrix, which states that $\Delta_{\text{CKM}} \equiv |V_{ud}|^2 + |V_{us}|^2 + |V_{ub}|^2 - 1$ should be zero. Current analyses show a $\approx 3\sigma$ tension with the SM [1–4] using the most precise value of $|V_{ud}|^2 = 0.94815(60)$ coming from $0^+ \to 0^+$ nuclear β decays [1], and $|V_{us}|^2 = 0.04976(25)$ obtained from kaon semileptonic decays ($K \to \pi \ell \nu_\ell$) along with the $N_f = 2+1+1$-flavor lattice result for $f_+^K(0)$ [5]. The estimate of $|V_{ub}|^2 \approx (2 \pm 0.4) \times 10^{-5}$ is too small to impact the unitarity test.

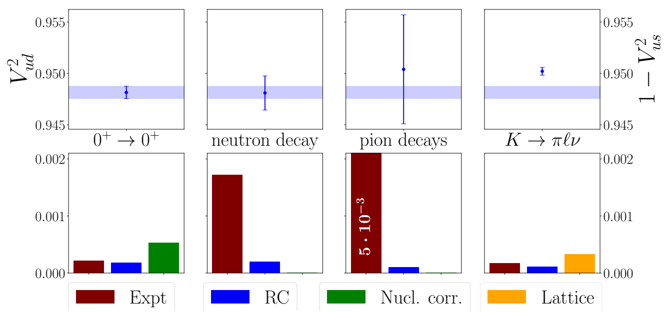

Figure 2: The error budgets on the various extractions of $|V_{ud}|^2$ and $|V_{us}|^2$ to test the unitarity of the first row of the CKM matrix [1, 6, 7].

A current analysis of the unitarity bound is shown in Fig. 1, with the errors from various sources in $0^+ \to 0^+$ nuclear, nucleon, pion and kaon decays shown in Fig. 2. While the extraction of V_{ud} from superallowed $0^+ \to 0^+$ nuclear decays is the best, it is still subject to significant uncertainty in the theoretical analysis of nuclear effects.

Theoretically, the neutron is a clean system, i.e., it has no uncertainty due to nuclear corrections. The largest theoretical uncertainty comes from the γW-box diagram illustrated in Fig. 3 for the pion as discussed in Refs. [8–10]. Lattice QCD can provide the least well determined non-perturbative part of the γW-box to reduce the uncertainty in the radiative corrections (RC) to neutron (and pion and kaon) decay. This, together with improvements in experiments measuring free neutron lifetime, τ_n, and the axial charge, g_A, will make the extraction of $|V_{ud}|^2$ from neutron decay competitive.

In this paper we present results for the pion and kaon (short for $K \to \pi\ell\nu_\ell$) decay as we have not yet obtained a precise signal in the neutron correlation functions. Nevertheless, we provide a brief review of the status of the extraction of $|V_{ud}|^2$ from neutron decay as it is the ultimate goal of this project. The analysis is carried out using the formula [4, 11]

$$|V_{ud}|^2 = \left(\frac{G_\mu^2 m_e^5}{2\pi^3} f\right)^{-1} \frac{1}{\tau_n(1+3g_A^2)(1+\text{RC})} = \frac{5099.3(3)\text{s}}{\tau_n(1+3g_A^2)(1+\text{RC})} \tag{1}$$

where g_A is best obtained from the neutron β decay asymmetry parameter A, G_μ is the Fermi constant extracted from muon decays, and $f = 1.6887(1)$ is a phase space factor. With future measurements of the neutron lifetime τ_n reaching an uncertainty of $\Delta\tau_n \sim 0.1$s, and of the ratio $\lambda = g_A/g_V$ of the neutron axial and vector coupling reaching $\Delta\lambda/|\lambda| \sim 0.01\%$, the extraction of V_{ud} with accuracy comparable to $0^+ \to 0^+$ superallowed β decay can be achieved provided the uncertainty in the RC to neutron decay can be reduced.

The lattice methodology for the calculation of RC to pion, kaon and neutron decays is similar [9, 10]. It requires the calculation of the γW-box diagram, illustrated in Fig. 3 for the pion. From here on, we restrict the discussion to pion ($\pi^+ \to \pi^0\ell\nu_\ell$) and kaon to pion ($K \to \pi\ell\nu_\ell$) semileptonic decays, for which the analogues of Eq. (1) to extract $|V_{ud}|^2$ and $|V_{us}|^2$ are [1, 12–14]

$$|V_{ud} f_+^\pi(0)|^2_{\pi\ell} = \frac{64\pi^3\,\Gamma_\pi}{G_\mu^2 M_\pi^5 I_\pi\,(1+\delta)} \tag{2}$$

$$|V_{us} f_+^K(0)|^2_{K\ell} = \frac{192\pi^3\,\text{BR}(K\ell)\,\Gamma_K}{G_\mu^2 M_K^5 C_K^2 S_{EW} I_{K\ell}\left(1+\delta_{EM}^{K\ell}+\delta_{SU(2)}^{K\ell}\right)}, \tag{3}$$

where $\Gamma_{\pi/K}$ are π and K decay rates, $I_{\pi,K}$ are known kinematic factors, $f_+^{\pi/K}$ are semileptonic form factors, C_K is a known normalization factor needed for kaon decay, S_{EW} is the short distance radiative correction, and the $\delta_{SU(2)}^{K\ell}$ is the isospin breaking correction. The two (long distance) radiative corrections in which the uncertainty needs to be reduced are δ for pion and $\delta_{EM}^{K\ell}$ for kaon decay.

Looking ahead, the experimental uncertainty in pion decay needs to be reduced by a factor greater than 20, at which point it will become roughly equal to that in radiative corrections. PIONEER [15] is a next generation experiment aimed at measuring precisely the rare pion decay branching ratios. Its primary goal is to improve the measurement of the branching ratio of the semileptonic decay by up to a factor of ten, thus reducing the experimental uncertainty in $|V_{ud}|^2$ by the same factor. At that point, as shown in Fig. 2, the experimental error in $|V_{ud}|^2$ from pion decay will become comparable to that from $0^+ \to 0^+$ superallowed nuclear decay, and also to the theory uncertainty.

In the determination of $|V_{us}|$ from kaon β decay, the largest uncertainty comes from $f_+^K(0)$

taken from lattice calculations [16]. Comparatively, the uncertainty in the radiative correction and experiments is already small [17].

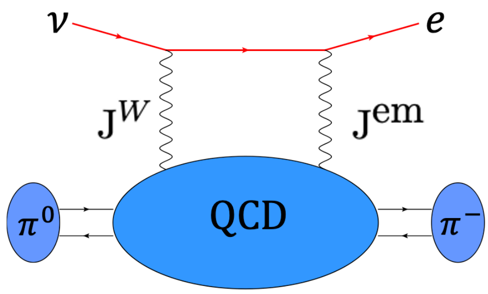

Figure 3: The $\gamma W-$ box diagram for RC to the pion decay.

This paper is organized as follows. The essential formulae needed to describe the calculation are summarized in the next section. The lattice setup is given in Sec. 3, error reduction methods used in the extraction of the hadronic tensor $\mathcal{H}^{VA}_{\mu\nu}$ in Sec. 4, a comparison of results for $\mathcal{M}_H(Q^2)$ with perturbation theory in Sec. 5, and extrapolation to the continuum limit in Sec. 6. The final results and comparison to previous calculations are given in Sec. 7.

2. Electroweak Box Diagram

Following the framework developed in [9, 18], the electroweak box diagram (called the axial γW diagram and shown in Fig. 4 (left)) is given by

$$\square^{VA}_{\gamma W}\Big|_H = \int_0^{+\infty} dQ^2 \int_{-Q}^{Q} dQ_0 \frac{1}{Q^4}\frac{1}{Q^2+M_W^2} \times \\ L^{\mu\nu}(Q,Q_0)T^{VA}_{\mu\nu}(Q,Q_0) \tag{4}$$

with H labeling the state, π, K or N, under consideration, and M_W the W meson mass and M_H the hadron mass. Substituting in the known leptonic part $L^{\mu\nu}(Q,Q_0)$ gives

$$\square^{VA}_{\gamma W}\Big|_H = -\frac{1}{F_+^H}\frac{\alpha_e}{\pi}\int_0^{\infty} dQ^2 \frac{m_W^2}{m_W^2+Q^2} \\ \times \int_{-\sqrt{Q^2}}^{\sqrt{Q^2}} \frac{dQ_0}{\pi}\frac{(Q^2-Q_0^2)^{\frac{3}{2}}}{(Q^2)^2}\frac{\epsilon_{\mu\nu\alpha\beta}Q_\alpha P_\beta T^{VA}_{\mu\nu}}{2M_H^2|\vec{Q}|^2}. \tag{5}$$

The hadronic tensor $T^{VA}_{\mu\nu}$ is given by

$$T^{VA}_{\mu\nu} = \frac{1}{2}\int d^4x\, e^{iQ\cdot x} \times \langle H_f(p)|T\left[J^{em}_\mu(0,0)J^{W,A}_\nu(\vec{x},t)\right]|H_i(p)\rangle\,, \tag{6}$$

where $J^{W,A}_\mu = Z_A\bar{u}\gamma_\mu\gamma_5 d$ and $J^{em}_\mu = Z_V(\frac{2}{3}\bar{u}\gamma_\mu d - \frac{1}{3}\bar{d}\gamma_\mu d)$ are the renormalized currents with Z_A and Z_V calculated in Ref. [19].

Only one term, T_3, in the expansion $T^{VA}_{\mu\nu} = i\epsilon_{\mu\nu\alpha\beta}q^\alpha p^\beta T_3 + \ldots$ of the spin-independent part of $T^{VA}_{\mu\nu}$ contributes [3, 9]. Knowing T_3 as a function of Q^2, the γW-box correction, using the notation in Refs. [9, 10], is given by

$$\square^{VA}_{\gamma W} = \frac{3\alpha_e}{2\pi}\int \frac{dQ^2}{Q^2}\frac{M_W^2}{M_W^2+Q^2}\mathcal{M}_H(Q^2) \tag{7}$$

with

$$\mathcal{M}_H\left(Q^2\right) = -\frac{1}{6}\frac{1}{F^H_+}\frac{\sqrt{Q^2}}{M_H}\int d^4x\,\omega(\vec{x},t) \times \epsilon_{\mu\nu\alpha 0}\, x_\alpha\, \mathcal{H}^{VA}_{\mu\nu}(\vec{x},t)\,, \tag{8}$$

$$\omega(t,\vec{x}) = \int_{-\frac{\pi}{2}}^{\frac{\pi}{2}} \frac{\cos^3\theta d\theta}{\pi}\frac{j_1\left(\sqrt{Q^2}|\vec{x}|\cos\theta\right)}{|\vec{x}|} \times \cos\left(\sqrt{Q^2}t\sin\theta\right)\,, \tag{9}$$

$$\mathcal{H}^{VA}_{\mu\nu}(\vec{x},t) = \langle H_f(p)|T\left[J^{em}_\mu(0,0)\,J^{W,A}_\nu(\vec{x},t)\right]|H_i(p)\rangle\,, \tag{10}$$

where j_1 in the weight function $\omega(t,\vec{x})$ is the spherical Bessel function. The calculation of the hadronic part $\mathcal{H}^{VA}_{\mu\nu}(\vec{x},t)$ with the insertion of vector (V) and axial (A) currents gives rise to, in general, four types of Wick contractions shown by the quark-line diagrams in Fig. 4 for pion decay. It is a function of the separation $\{\vec{x},t\}$, and on the lattice, the integral becomes a sum. As can be seen from Eq. (10), $\mathcal{M}_H\left(Q^2\right)$ is however, available for all values of Q^2. One expects the signal in $\mathcal{H}^{VA}_{\mu\nu}(\vec{x},t)$ to fall off with $\{\vec{x},t\}$, and in Fig. 5, we show that the integral saturates for $R^2 \gtrsim 2\text{fm}^2$. To be conservative and save computation time, we choose the integration volume to be larger than $R^2 \sim 3.3\text{fm}^2$ on all the ensembles.

3. Lattice Setup

The calculation has been performed using eight $N_f = 2+1+1$ highly improved staggered quark (HISQ) ensembles generated by the MILC collaboration [20], whose parameters are given in Table 1, and shown in the $\{a, M_\pi\}$ plane in Fig. 6. For comparison, we also show the parameters in the "Iwasaki" and "DSDR" variants of domain-wall fermions used in Ref. [9].

The correlation functions are constructed using Wilson-clover fermions, and the tuning of the light quark mass in the isosymmetric limit is done by requiring $M_\pi^{\text{valence}} = M_\pi^{\text{sea}}$ as described in

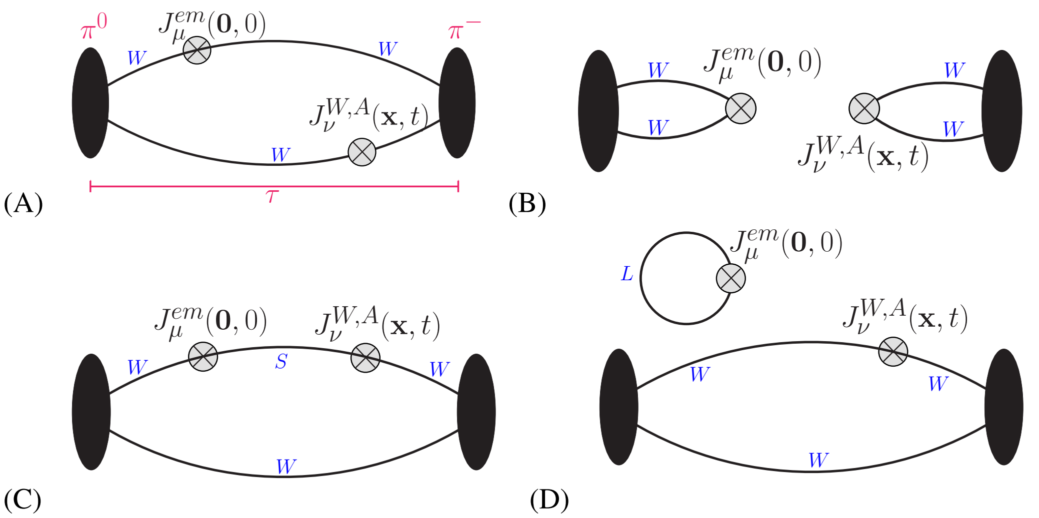

Figure 4: The four quark-line diagrams that contribute to the pion γW-box quantity $\mathcal{H}^{VA}_{\mu\nu}(\vec{x},t) = \langle\pi|\mathrm{T}[J^{em}_\mu(x)J^{W,A}_\nu(0)]|\pi\rangle$ (right).

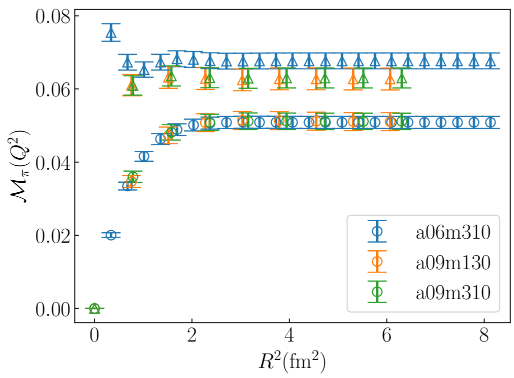

Figure 5: The dependence of $\mathcal{M}_\pi$ on R^2 to check convergence. (See Section 2 for details.) Circles are used for $Q^2 = 0.317$ GeV^2 and triangles for $Q^2 = 3.0$ GeV^2 data.

Ref. [19] and their values are given in Table 1. The strong coupling α_s at each lattice ensemble was computed using fourth order perturbative expression [21] with $\Lambda^{n_f=4}_{\mathrm{QCD}} = 292$ MeV taken from [22].

Of the four quark-line diagrams shown in Fig. 4, diagrams are A and C are called "connected". The "disconnected" diagram (B) does not contribute due to the γ_5-hermiticity property of the quark propagator, and diagram (D) vanishes in the SU(3) limit. This calculation has not been done at the SU(3) point, nevertheless we neglect diagram (D) assuming it is small. Under the same assumption, we also neglect contributions of the charm quark. To construct these correlation functions, quark propagators are generated using wall sources at two ends of a sublattice with separation τ in time (see Table 1). We label these quark lines by W. For the internal line S in diagram C, we solve for an additional propagator from the position of the vector current V_μ placed on the middle timeslice between the source and sink. This point is labeled $\{\vec{x} = 0, t = 0\}$. We choose 256 such points for diagram A and 64 for diagram C. Data are collected with the position of A_μ varied within distance

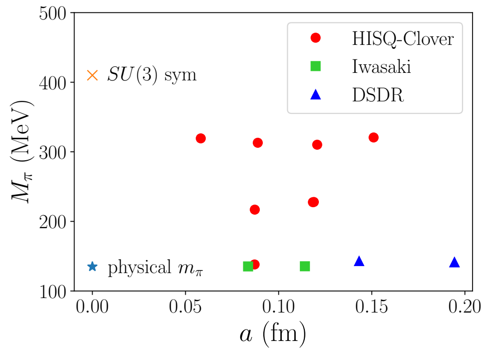

Figure 6: The lattice spacing and pion mass of the eight ensembles (red circles) with 2+1-flavors of Wilson-clover fermions analyzed in this study. The physical point (Star) and SU(3) symmetric point (Cross) are also shown. We also show the points for DSDR (Triangle) and Iwasaki (Square) actions that were used in Feng. et al [9, 10].

R^2, listed in Table 1, from these points. On each configuration, we use 8 regions (sublattices) offset by $N_T/8$ on which we repeat the calculation to further increase the statistics. With the current statistics, the errors in the data from the eight ensembles are comparable as shown later in Fig. 11. Since the total error budget for the box diagram is already dominated by the uncertainty in the renormalization constant Z_A as shown in Fig. 7, the current statistics are considered sufficient.

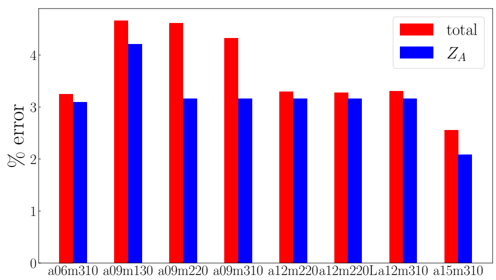

Figure 7: Fractional error in the calculation of the box diagram for the pion on the eight ensembles. The total uncertainty (red bar) in the calculation is dominated by the uncertainty from the renormalization constant Z_A (blue bar).

In Fig. 8, we show the result for $\mathcal{M}_H$ and the γW-box as a function of the separation τ between the wall source and sink. Our data show no significant dependence on $\tau > 2.4$ fm, at which separation only the ground state of the pseudoscalar mesons contributes to the calculation. To be conservative and because the signal in correlation functions for pseudoscalar mesons does not degrade with τ, we chose to work with τ in the range $[3.48 \leq \tau \leq 3.63]$ fm on all ensembles. Note that this ability to choose τ large enough to isolate the ground state is special to pseudoscalar mesons. For our target case of neutrons, the signal decays exponentially and excited state contamination may be a severe challenge [23]. As a result, even with much larger statistics, our ongoing calculations for neutrons have not yet yielded a statistically significant signal.

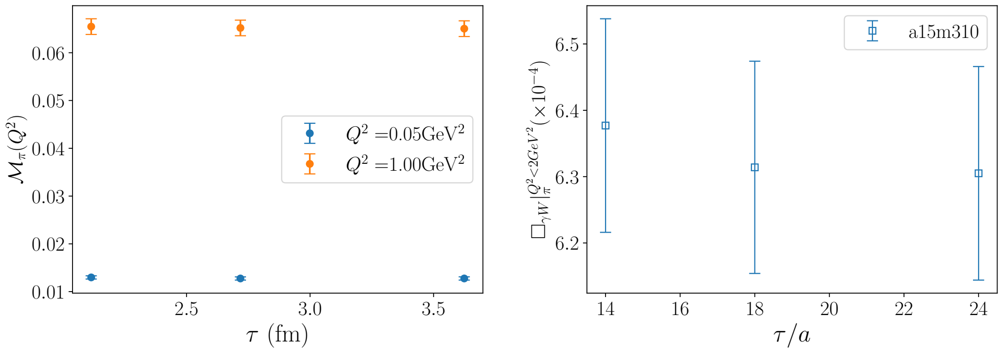

Figure 8: The data for $\mathcal{M}_\pi(Q^2)$ and the γW-box contribution on the $a15m310$ ensemble show no significant dependence on the source-sink separation τ. We chose to perform all analyses in this paper with τ in the range $[3.48 \le \tau \le 3.63]$ fm.

Ensemble ID	a[fm]	α_S	$M_\pi^{\rm val}$	$M_\pi^{\rm sea}$	$L^3 \times T$	$M_\pi L$	τ/a	$R^2(\text{fm}^2)$	N_{conf}
a06m310	0.0582(04)	0.2433	319.3(5)	319.3(5)	$48^3 \times 144$	4.52	62	5.42	168
a09m130	0.0871(06)	0.2871	138.1(1.0)	128.2(1)	$64^3 \times 96$	3.90	40	6.07	45
a09m220	0.0872(07)	0.2873	225.9(1.8)	220.3(2)	$48^3 \times 96$	4.79	40	6.07	93
a09m310	0.0888(08)	0.2897	313.0(2.8)	312.7(6)	$32^3 \times 96$	4.51	40	6.31	156
a12m220	0.1184(09)	0.3348	227.9(1.9)	216.9(2)	$32^3 \times 64$	4.38	30	5.61	150
a12m220L	0.1189(09)	0.3348	227.6(1.7)	217.0(2)	$40^3 \times 64$	5.49	30	5.65	150
a12m310	0.1207(11)	0.3384	310.2(2.8)	305.3(4)	$24^3 \times 64$	4.55	30	5.83	179
a15m310	0.1510(20)	0.3881	320.6(4.3)	306.9(5)	$16^3 \times 48$	3.93	24	9.12	80

Table 1: Description of the eight HISQ ensembles used in this work. To increase the statistics, we create, on each configuration, 8 sublattices and in each make 256 measurements for diagram A and 64 for diagram C. The values of $M_\pi^{\rm val}$ and $M_\pi^{\rm sea}$ are in MeV. The values of a, $M_\pi^{\rm sea}$ and $M_\pi^{\rm val}$ are reproduced from Ref. [19].

4. Error reduction in the extraction of $\mathcal{H}_{\mu\nu}^{VA}$

We can calculate the ratios [24]

$$\frac{\mathcal{H}_{\mu\nu}^{VA}(t,\vec{x})}{F_+^\pi} = 2M_\pi \frac{C_{4pt}(\tau,t,\vec{x})}{\sqrt{2}C_{3pt}(\tau)} \tag{11}$$

$$\frac{\mathcal{H}_{\mu\nu}^{VA}(t,\vec{x})}{F_+^K} = 2M_K \frac{C_{4pt}(\tau,t,\vec{x})}{C_{3pt}(\tau)} \tag{12}$$

using the ratio of correlation functions in the right hand side of Eq. (12).

5. Comparing lattice results for $\mathcal{M}_H(Q^2)$ with perturbation theory

As mentioned in Sec. 2, $\mathcal{M}_H$ can be extracted at all values of Q^2. In practice, we choose sixty Q^2 values that are the same on all eight ensembles with a higher density below $Q^2 < 1$ GeV^2. Data at these 60 points are converted into the smooth curves shown in Fig. 9 (top) using the cubic spline interpolator from scipy library [25]. Data show that as Q^2 increases above 1 GeV^2, the value of $\mathcal{M}_H$

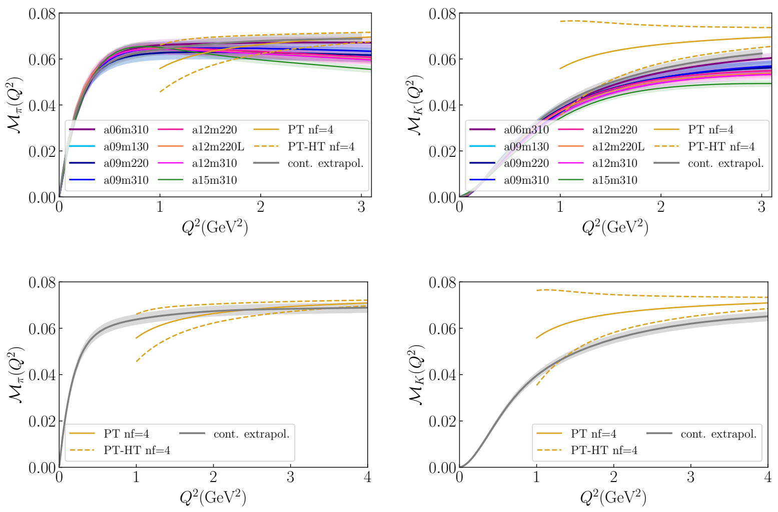

Figure 9: $M_H(Q^2)$ for the (a) pion and (b) the Kaon for the eight ensembles (top). The bottom panels zoom in on the comparison between the grey band obtained by making a continuum extrapolation at each of the 60 Q^2 values and the gold line shows the perturbative result with uncertainty band reflecting higher-twist corrections.

on coarser lattices decreases, indicating a dependence on the lattice spacing. Below $Q^2 < 1$ GeV^2, the trend reverses. The integrated box contributions for $Q^2 < 2$ GeV^2 and their dependence on a and M_π^2 is shown in Fig. 10.

To compare the $\mathcal{M}_H(Q^2)$ from lattice and perturbation theory, we extrapolate the data to the continuum limit at $M_\pi = 135$ MeV using a fit linear in $\alpha_S\, a$ since the dependence on M_π is observed to be small (See Fig. 11). These fits, for all the ensembles and all Q^2 values, have a p-value above 0.2. As shown in Figure 9, this continuum limit data, represented by the grey solid line, roughly agrees with the perturbative result obtained using the operator product expansion [9, 26, 27] (gold line) for $Q^2 > 2$GeV^2. Uncertainty in the perturbative result arises from the truncation of the series at the 4$^{\text{th}}$ order and the neglected higher-twist (HT) contributions [9]. Since diagram (A) only has HT contributions, we use its full lattice value as an estimate of the HT uncertainty and show this by the dotted lines about the perturbative result.

6. Continuum extrapolation of the lattice data

The extrapolation of the γW-box for $Q^2 < Q^2_{\text{cut}}$ to the continuum limit $a = 0$ and pseudoscalar mass $M_\pi = M_\pi^{\text{phys}}$ for the pion, and $M_\pi = M_K^{\text{SU(3)}}$ for the kaon is carried out keeping the lowest order dependence on the pion mass, M_π^2, and on the lattice spacing, $\alpha_S\, a$:

$$\Box|_{VA}^{Q^2<Q^2_{\text{cut}}}(M_\pi, a) = c_0 + c_1 \alpha_S\, a + c_2 M_\pi^2 \,. \tag{13}$$

This extrapolation is shown in (Fig. 10) and gives

$$\Box_{\gamma W}^{VA}|_\pi^{Q^2\le 2\text{GeV}^2} = 0.651(25) \times 10^{-3} \,, \tag{14}$$

$$\Box_{\gamma W}^{VA}|_K^{Q^2\le 2\text{GeV}^2} = 0.230(15) \times 10^{-3} \,, \tag{15}$$

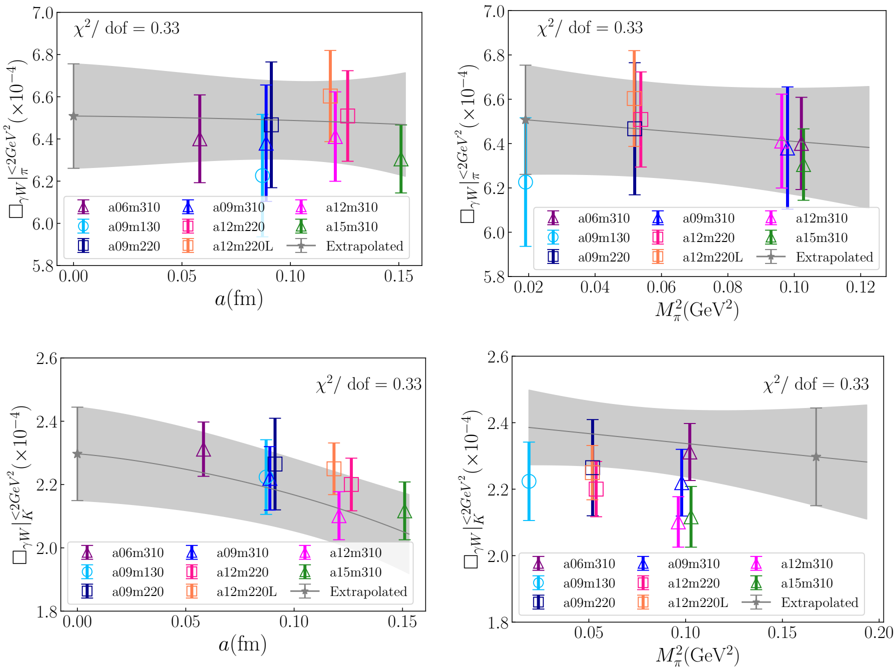

Figure 10: The dependence of the γW-box contribution for $Q^2 \leq 2\text{GeV}^2$ for the pion (top) and kaon (bottom) decay on the lattice spacing a (left), and the pion mass (M_π^2) (right). The symbols for the various ensembles are defined in the inset and in Table 1. The physical point result given by the simultaneous fit in a and M_π^2 (grey band) is shown by the grey star symbol. The result for the kaon is evaluated at the SU(3) symmetric point.

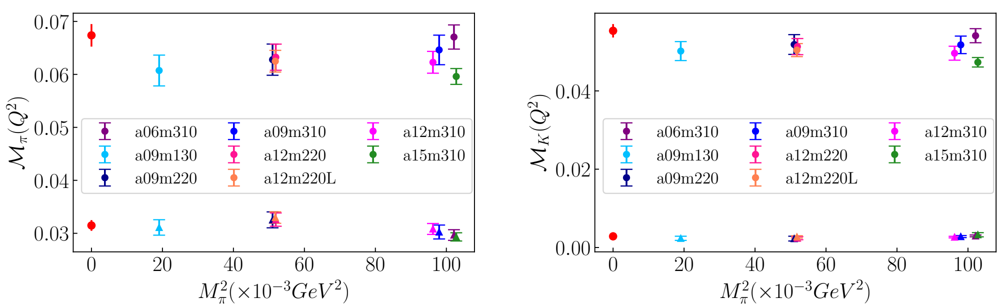

Figure 11: $\mathcal{M}_H(Q^2)$ for the pion (left) and kaon (right) at $Q^2 = 0.133$ GeV^2 (triangles), 2.00 GeV^2 (circles). Ensembles are labeled by color. Data for $\mathcal{M}_H(Q^2)$ do not show a significant dependence on M_π^2. The red points on the very left are the continuum extrapolated values using a fit linear in $a\alpha_S$, i.e., ignoring possible dependence on M_π^2.

Systematic uncertainties due to the chiral-continuum extrapolation are included in these estimates. We also estimated possible uncertainty in $\mathcal{M}_H$ due to integration using 52 discrete points in Q^2 as the difference between using the trapezoid and Simpson methods and found it to be negligible. We assume finite volume effects are negligible since all the ensembles have $M_\pi L \geq 3.9$.

7. Results for the γW-box diagram and comparison to earlier works

The contribution above the energy cut at $Q^2 = 2\,\mathrm{GeV}^2$ is computed using the operator product expansion [9] with the higher-twist uncertainty estimated using diagram A (See Fig. 4).

$$\square^{VA}_{\gamma W}|^{Q^2>2\mathrm{GeV}^2}_{\pi,K} = 2.159(6)_{HO}(7)_{HT} \times 10^{-3}. \tag{16}$$

Combining Eq. (16) with Eq. (15) gives our results for the full box contribution:

$$\square^{VA}_{\gamma W}|_\pi = 2.810(26) \times 10^{-3}\,, \tag{17}$$

$$\square^{VA}_{\gamma W}\Big|_{K^0,SU(3)} = 2.389(17) \times 10^{-3}\,, \tag{18}$$

which are in good agreement with those obtained by Feng et al. [9, 10]:

$$\square^{VA}_{\gamma W}|_\pi = 2.830(11)(26) \times 10^{-3}\,, \tag{19}$$

$$\square^{VA}_{\gamma W}\Big|_{K^0,SU(3)} = 2.437(44) \times 10^{-3}\,. \tag{20}$$

The difference in $\square^{VA}_{\gamma W}\Big|_{K^0,SU(3)}$ is 1.02σ, but note that our value is determined with extrapolation in M_π^2 to $SU(3)-$symmetric point, while the Feng et al. value, also called $\square^{VA}_{\gamma W}|_{K^0,SU(3)}$, was computed at the physical pion mass in all five ensembles, i.e., without extrapolation to $M_K|_{\mathrm{SU}(3)}$.

The agreement between the two calculations provides an important consistency check as they are done at different values of $\{a, M_\pi\}$ (see Fig. 6) and with different lattice actions. The largest uncertainty in the results presented in [9, 10] comes from the systematic difference between DSDR and Iwasaki estimates, whereas in our calculation it comes from the renormalization constant Z_A as shown in Fig. 7, which is unity for domain-wall fermions.

Our data from the eight ensembles, all with the same action, provide a more controlled chiral-continuum extrapolation than in [9, 10]. The data for the pion display no significant dependence on a or M_π^2. The data for the kaon in Fig. 10 shows $\approx 10\%$ dependence on a but is flat with respect to M_π^2. A similar level of dependence on a was found in the Iwasaki action data in Ref. [10].

To conclude, taking the two calculations together increases our confidence that lattice QCD calculations of the non-perturbative part of the radiative corrections to pion and kaon decays given by the γW-box are robust. The analysis of RC to neutron decays is, as expected, more challenging because of the exponentially decaying signal-to-noise problem and the need to remove possibly large contributions from excited states.

Acknowledgments

We thank the MILC collaboration for providing the HISQ lattices, and Vincenzo Cirigliano and Emanuele Mereghetti for discussions. The calculations used the CHROMA software suite [28]. Simulations were carried out at (i) the NERSC supported by DOE under Contract No. DE-AC02-05CH11231; (ii)the Oak Ridge Leadership Computing Facility, which is a DOE Office of Science User Facility supported under Award No. DE-AC05-00OR22725 and was awarded through the INCITE program project HEP133, (iii) the USQCD collaboration resources funded by DOE HEP, and (iv) Institutional Computing at Los Alamos National Laboratory. This work was supported by LANL LDRD program and TB and RG were also supported by the DOE HEP under Contract No. DE-AC52-06NA25396.

References

[1] Particle Data Group collaboration, *Review of Particle Physics*, *PTEP* **2022** (2022) 083C01.

[2] C.-Y. Seng, M. Gorchtein, H.H. Patel and M.J. Ramsey-Musolf, *Reduced Hadronic Uncertainty in the Determination of V_{ud}*, *Phys. Rev. Lett.* **121** (2018) 241804 [1807.10197].

[3] C.Y. Seng, M. Gorchtein and M.J. Ramsey-Musolf, *Dispersive evaluation of the inner radiative correction in neutron and nuclear β decay*, *Phys. Rev.* **D100** (2019) 013001 [1812.03352].

[4] A. Czarnecki, W.J. Marciano and A. Sirlin, *Radiative Corrections to Neutron and Nuclear Beta Decays Revisited*, *Phys. Rev.* **D100** (2019) 073008 [1907.06737].

[5] Flavour Lattice Averaging Group (FLAG) collaboration, *FLAG Review 2021*, *Eur. Phys. J.* **C82** (2022) 869 [2111.09849].

[6] UCNτ collaboration, *Improved neutron lifetime measurement with UCNτ*, *Phys. Rev. Lett.* **127** (2021) 162501 [2106.10375].

[7] J.C. Hardy and I.S. Towner, *Superallowed* 0+ $\rightarrow$ 0+ *beta-decay from* $Tz = -1$ *sd-shell nuclei*, *Journal of Physics: Conference Series* **387** (2012) 012006.

[8] A. Sirlin, *Current Algebra Formulation of Radiative Corrections in Gauge Theories and the Universality of the Weak Interactions*, *Rev. Mod. Phys.* **50** (1978) 573.

[9] X. Feng, M. Gorchtein, L.-C. Jin, P.-X. Ma and C.-Y. Seng, *First-principles calculation of electroweak box diagrams from lattice QCD*, *Phys. Rev. Lett.* **124** (2020) 192002 [2003.09798].

[10] P.-X. Ma, X. Feng, M. Gorchtein, L.-C. Jin and C.-Y. Seng, *Lattice QCD calculation of the electroweak box diagrams for the kaon semileptonic decays*, *Phys. Rev.* **D103** (2021) 114503 [2102.12048].

[11] A. Czarnecki, W.J. Marciano and A. Sirlin, *Neutron lifetime and axial coupling connection*, *Phys. Rev. Lett.* **120** (2018) 202002.

[12] V. Cirigliano, M. Knecht, H. Neufeld and H. Pichl, *The Pionic beta decay in chiral perturbation theory*, *Eur. Phys. J. C* **27** (2003) 255 [hep-ph/0209226].

[13] D. Pocanic et al., *Precise measurement of the pi+ —> pi0 e+ nu branching ratio*, *Phys. Rev. Lett.* **93** (2004) 181803 [hep-ex/0312030].

[14] A. Czarnecki, W.J. Marciano and A. Sirlin, *Pion beta decay and Cabibbo-Kobayashi-Maskawa unitarity*, *Phys. Rev.* **D101** (2020) 091301 [1911.04685].

[15] PIONEER collaboration, W. Altmannshofer et al., *PIONEER: Studies of Rare Pion Decays*, 3, 2022.

[16] Flavour Lattice Averaging Group (FLAG) collaboration, *FLAG Review 2021*, *Eur. Phys. J.* **C82** (2022) 869 [2111.09849].

[17] C.-Y. Seng, D. Galviz, W.J. Marciano and U.-G. Meißner, *Update on |Vus| and |Vus/Vud| from semileptonic kaon and pion decays*, *Phys. Rev.* **D105** (2022) 013005 [2107.14708].

[18] C.-Y. Seng, M. Gorchtein and M.J. Ramsey-Musolf, *Dispersive evaluation of the inner radiative correction in neutron and nuclear β decay*, *Phys. Rev. D* **100** (2019) 013001.

[19] R. Gupta, Y.-C. Jang, B. Yoon, H.-W. Lin, V. Cirigliano and T. Bhattacharya, *Isovector Charges of the Nucleon from 2+1+1-flavor Lattice QCD*, *Phys. Rev.* **D98** (2018) 034503 [1806.09006].

[20] MILC Collaboration collaboration, *Lattice QCD ensembles with four flavors of highly improved staggered quarks*, *Phys. Rev.* **D87** (2013) 054505 [1212.4768].

[21] A. Deur, S.J. Brodsky and G.F. de Teramond, *The QCD Running Coupling*, *Nucl. Phys.* **B90** (2016) 1 [1604.08082].

[22] Particle Data Group collaboration, *Review of Particle Physics*, *Chin. Phys. C* **40** (2016) 100001.

[23] Nucleon Matrix Elements (NME) collaboration, *Precision nucleon charges and form factors using (2+1)-flavor lattice QCD*, *Phys. Rev. D* **105** (2022) 054505 [2103.05599].

[24] J.-S. Yoo, T. Bhattacharya, R. Gupta, S. Mondal and B. Yoon, *Electroweak box diagram contribution for pion and kaon decay from lattice QCD*, *Phys. Rev. D* **108** (2023) 034508 [2305.03198].

[25] P. Virtanen, R. Gommers, T.E. Oliphant, M. Haberland, T. Reddy, D. Cournapeau et al., *SciPy 1.0: Fundamental Algorithms for Scientific Computing in Python*, *Nature Methods* **17** (2020) 261.

[26] S.A. Larin and J.A.M. Vermaseren, *The alpha-s**3 corrections to the Bjorken sum rule for polarized electroproduction and to the Gross-Llewellyn Smith sum rule*, *Phys. Lett. B* **259** (1991) 345.

[27] P.A. Baikov, K.G. Chetyrkin and J.H. Kuhn, *Adler Function, Bjorken Sum Rule, and the Crewther Relation to Order α_s^4 in a General Gauge Theory*, *Phys. Rev. Lett.* **104** (2010) 132004 [1001.3606].

[28] SciDAC Collaboration, LHPC Collaboration, UKQCD Collaboration collaboration, *The Chroma software system for lattice QCD*, *Nucl. Phys. Proc. Suppl.* **140** (2005) 832 [hep-lat/0409003].